# CORRECTION OF MOTION ARTEFACTS IN HR-PQCT USING CYCLE-CONSISTENT ADVERSARIAL NETWORKS

Philipp Y. Steiner (1), Matthias Walle (1,2), Mattia Rigotti (2), Danielle E. Whittier (1), Cael McLennan (1), Penny R. Atkins (1), Ralph Müller (1), Caitlyn J. Collins (1,3)

1. Institute for Biomechanics, ETH Zurich, Zurich, Switzerland; 2. IBM Research Zurich, Rüschlikon, Switzerland, 3. Department for Biomedical Engineering and Mechanics, Virginia Tech, Blacksburg, USA.

## Introduction

High-resolution peripheral quantitative computed tomography (HR-pQCT) can provide important information about age-related changes in bone microstructure and strength [1]. However, in elderly patients, uncontrollable tremors often induce motion artefacts that affect the accuracy of HR-pQCT measurements [2]. Repeat acquisition protocols are commonly used to address this issue; nevertheless, they are ineffective in these patients, resulting in motion-blurred and streaked images. Deblurring these scans computationally is a severely ill-posed inverse problem. Therefore, we present a deep learning approach to suppress motion-induced artefacts in HR-pQCT scans.

## Methods

HR-pQCT scans of 13 patients scanned biweekly for five weeks (XtremeCT II, Scanco Medical, 60.7 µm, 68 kV, 1470 µA, 43 ms) were obtained from a previous study [3]. Motion scores of all scans were assessed on a scale of 1 (no visible motion artefacts) to 5 (major streaks) [1]. Scans with a score of 1 were classified as high-quality (HQ), while those with a score 2 or less were classified as low-quality (LQ). 15 LQ-HQ scan pairs were 3D registered and divided patient-wise into 80% train, 10% test, and 10% validation datasets. Our filtering approach used a generative adversarial network (cycle-GAN) as the building block [4]. It enforced the cycle consistency using the least absolute deviation (L1) to establish a nonlinear end-to-end mapping from LQ input images to denoised and deblurred HQ outputs. To quantify the signal recovery after motion-filtering, we calculated a signal-to-noise ratio (SNR) by fitting two Gaussian distributions to values corresponding to bone (signal) and soft-tissue (noise). Further, a peak-SNR and structural similarity index were calculated between LQ, HQ and filtered LQ pairs to assess degradations of structures within the image. Finally, three blinded operators evaluated motion scores of the validation dataset in random order. Fleiss' kappa ($\kappa$) was used to assess inter-rater reliability between operators before and after filtering.

## Results

We found structural similarity index (0.67±0.03) and peak-SNR (21.43±1.03) were not significantly different between LQ and HQ images. However, the mean SNR was significantly higher in HQ (15.83±1.10) compared to LQ (13.49±0.91, $p<0.01$), promoting SNR as an evaluation target. Our motion-filtering approach consistently improved the SNR of LQ images to 15.39±0.92 ($p<0.01$, Fig. 1A), comparable to that of HQ (15.83±1.10). Visually, images were denoised and deblurred; yet, the network failed to resolve severe artefacts (cortical breaks). Finally, operators graded LQ images better (Fig. 1B) and more consistently after motion-filtering, with $\kappa$ increasing from 0.162 to 0.237.

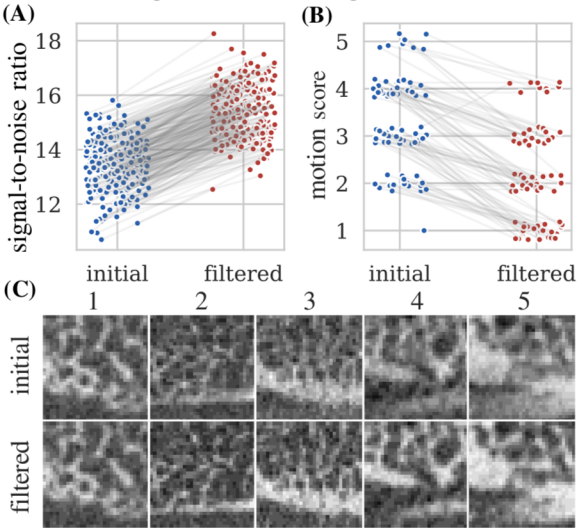


*Fig. 1: SNR (A), motion score (B), and visual (C) improvement of validation data after motion-filtering.*

## Discussion

Using paired *in vivo* scan-rescan data, the proposed cycle-GAN method produced promising results in preserving anatomical information and suppressing moderate motion artefacts in HR-pQCT images after acquisition. Severe degradations, causing breaks in the cortex, were not fully resolved, but visual evaluations confirmed that our proposed method improves image quality. Future studies should assess how this method impacts the diagnostic quality of density and morphology measures. Overall, this work offers stakeholders a realistic methodology for improving current HR-pQCT datasets such that tools for analysing trabecular structure can be used more effectively.

## References

1. Whittier DE et al., Osteoporos Int. 31(9):1607-27, 2020.
2. Crawford CR, King KF, Med. Phys. 17(6):967-82, 1990.
3. Atkins PR et al., JBMR Plus 5(6):e10493, 2021.
4. Zhu JY et al., IEEE Comp. Vis. pp. 2223-2232, 2017.

**Acknowledgements:** Support from EU-H2020 (860898 and 841316) and SNF (320030L_170205). PS and MW contributed equally to this work.